3-D LDV MEASUREMENTS IN SWIRLING TURBULENT PIPE FLOW

**Venkatesa I. Vasanta Ram, Gerta Rocklage-Marliani,
Thomas Demmer and Maren Schmidts**

Institut für Thermo- und Fluiddynamik
Ruhr-Universität Bochum
D-44780 Bochum, Germany

ABSTRACT

The present work is an experimental study of the evolution of swirl with the well defined characteristic of solid-body rotation introduced at an initial station into the turbulent flow in a pipe. The swirl is generated by a specially designed device based on the principle of a rotating honeycomb so that the experimentally realised flow exhibits the characteristic of solid-body rotation over essentially the whole pipe cross section. The evolution of the various components of the mean velocity vector and Reynolds stress tensor in this flow is measured by 3-D LDV employing the refractive index matching technique at rotation numbers of up to one. The results draw attention to some outstanding features of the turbulence in this flow.

INTRODUCTION

Swirl in a flow, a term which we use here to denote a flow with streamlines wound in the shape of a helix, is a common phenomenon occuring both in nature and in engineering. The cause of swirl in a flow may be traced to several kinds of source and these may be conveniently classified under two broad headings. Firstly, swirl may be purposely introduced across boundaries into the flow and this is often done in engineering practice through devices such as vanes or jets blowing tangentially to the mainstream direction. Secondly, swirl may also arise inadvertantly of its own due an inherent mechanism of instability within the flow, a mechanism activated when the angular momentum in the flow is distrubuted suitably and the relevant flow parameters lie in a certain range. Görtler vortices in the boundary layer on a concave wall are an example for the origin of swirl through the instability mechanism. In a given flow situation it is of course possible that both kinds of mechanism are simultaneously present. The helical winding of the streamlines in a flow with swirl implies the streamline curvature not lying entirely in one plane, and this is an outstanding topological feature of these flows. Experiments hitherto conducted in swirling flows have drawn attention to anomalous behaviour of some observed turbulence quantities hierin (see eg. Kitoh, 1991), a reason for which is conjectured to be the prevalent non-planar streamline curvature. One such observation of far reaching consequence is regarding the relative orientation of the principal axes of the Reynolds stress tensor and the strain rate tensor. The experiments hint that these may not coincide with each other in the entire flow region, which is a possible explanation for the failure of some turbulence models working with the concept of an eddy viscosity to capture certain salient features of these flows. Evidence for such a failure of turbulence models may be found, for example, in Hogg and Leschziner (1989). The resolution of questions connected herewith would call for a thorough measurement of the velocity vector and the Reynolds stresses in a set of suitably designed experiments that qualify to be regarded as bench marks and this has been the motivation of the present work. In order to meet the standards set for bench marks the experiment was designed to generate swirl with the well defined characteristic of solid-body rotation at an initial section over a broad range of the flow parameter describing swirl, let it evolve downstream under carefully monitored experimental conditions, and follow the flow development with suitable non-intrusive instrumentation. The last was necessary due to the reported extreme sensitivity of swirling flows to probes, see eg. Escudier (1987). The aim of the work was to gather experimental data and to analyse the steps of flow development with the support of a theoretical framework to shed light on the physical mechanisms of generation and maintenance of turbulence in a swirling flow.

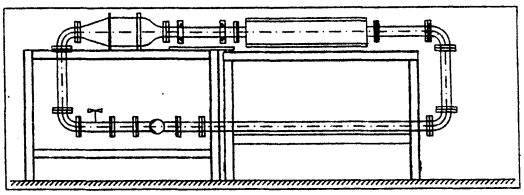

Figure 1: The experimental facility

3-D LDV measurements have been conducted in a specially designed facility in which a "rotating honeycomb" generates at an initial station a swirling flow with solid-body rotation to a high degree of accuracy over a wide range of rotation numbers. This flow evolves down-

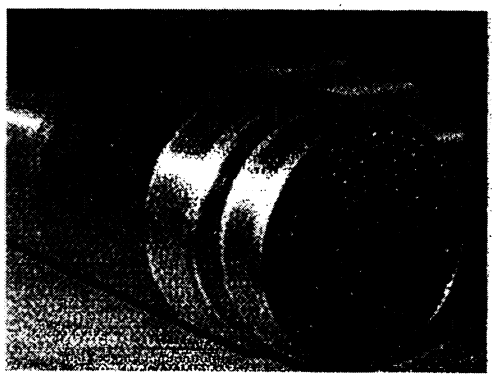

Figure 2: The swirl generator

stream under the influence of turbulence that establishes itself in the flow. In order to circumvent the difficulties associated with carrying out 3-D LDV-measurement of flows in geometries with curved walls, the facility operates on the principle of refractive-index matching of the fluid and the surroundings (Budwig, 1994). The facility and instrumentation are described in the following section. A selection of the results of measurement is presented in the subsequent section.

THE EXPERIMENTAL FACILITY AND EXPERIMENTS

A schematic diagram of the facility built is shown in fig. 1. Its test section is a 1500 mm long pipe of inner diameter 100 mm which is enclosed in a box with plane walls. Both the pipe and the surrounding box are made out of glass with a refractive index of 1.4730. The working fluid in the facility is a mixture of Cumol and paraffin in the ratio 78.29% by volume to 21.71%. In this ratio the mixture has a refractive index of 1.4730, a density of 835 kg/m^3 and a dynamic viscosity of 1.07$\cdot$ 10^{-3} PaS, all the fluid property values being given at a temperature of 20 C. It may be noted that the density and viscosity are close to values of water. The space between the test section and the box is also filled with the same working fluid so that light refraction takes place only at the plane walls of the box and not at the curved walls of the pipe. A thermostat is built into the facility to maintain constancy of temperature.

Fig. 2 shows a photograph of the swirl generator. It consists of a steel pipe, 500 mm long and 100 mm inner diameter, into which commercially available thin-walled (0.2 mm) precision steel tubes of 4 mm diamter and 500 mm length were packed as tightly as possible. Care was taken during fabrication that the tubes remained axial so as to assure that no swirl is introduced by the apparatus itself into the flow when the swirl generator was not set in rotation. The void space between the tubings was filled up with resin. The pipe could be rotated about its own axis at speeds varying from 100 to 800 rpm. The design principle of our present swirl generator is thus the same as in Anwer and So (1989) and Leuchter et al (1991), but differs from these in matters of constructional detail.

The facility was designed and built to use a commercially available 3-D LDV-system of DANTEC available in our laboratory, see Kiel (1995). The system is equipped with burst spectrum analysers (BSA). Several modifications of the equipment as a whole to improve upon the ease of operation and accuracy at traversing, at determining the location of the measuring volume and seeding to obtain enhanced data rates were carried out to adapt the system for the liquid flow measurement in the present work and these are described in Rocklage-Marliani (1998).

All the experiments reported in this work were conducted at a nominal Reynolds number of 2.8$\cdot$10^5, where the pipe diameter and the through-flow bulk velocity are the reference quantities of length and velocity respectively. The rotation numbers, defined as the angular velocity of the swirl generator referred to the pipe radius and the bulk velocity, were 0, 0.25, 0.5, 0.75 and 1.0.

RESULTS AND DISCUSSION

Due to limitations of space we present herein only a representative sample of the results covering axial and azimuthal velocities and Reynolds stresses. Field measurements of these quantities, i.e. measurements over the entire cross section, did not indicate any absence of rotational symmetry, so it suffices to show profiles along a radius only.

The measured profiles of axial and azimuthal velocities along a radius at the three axial stations are given in Fig. 3. The axial velocity profiles clearly show a bulge evolving downstream which is more pronounced at higher rotation numbers. In other words, an initially convex velocity profile develops a point of inflection as the flow evolves downstream. The profiles also show that the azimuthal velocity distribution corresponds to solid body rotation over a core, a feature often observed in swirling flows. However, in the present experiment, the core size seems to be large compared to flows with other forms of swirl generation, eg. Kitoh (1991). Furthermore, the angular velocity in the core undergoes little streamwise modification in the streamwise region studied, i.e. 14D, this feature again being more pronounced at higher rotation numbers. The distribution of the azimuthal velocity according to solid-body rotation permits a clear delineation of the core from the periphery from the experimental data. The radial position of the periphery thus defined at the three streamwise locations of $x/D = 4$, 9 and 14 for the 4 non-zero rotation numbers studied is given in Table 1. The Reynolds stress measurements at the rotation number of 0.5 shown in fig. 4 are representative of the evolution of this quantity in the

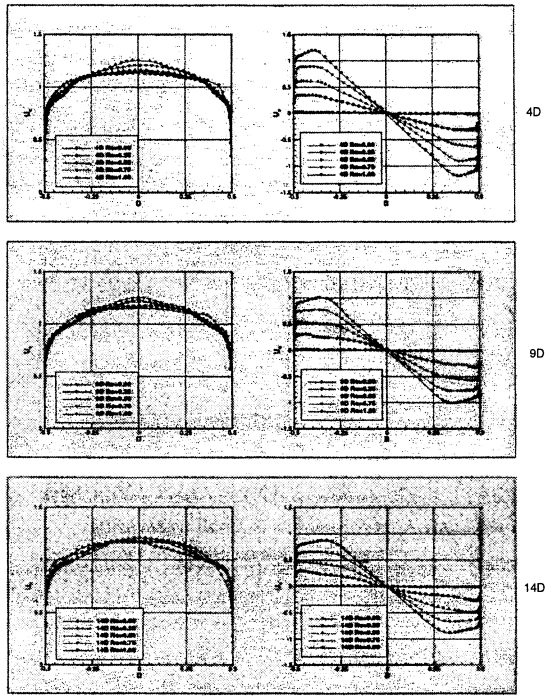

Figure 3: Measured axial and azimuthal velocities

X		Ro=0,25	Ro=0,50	Ro=0,75	Ro=1,00
4D	R_C	-	-	-	-
4D	R_{core}	0,733	0,493	0,733	0,733
4D	R_{bl}	0,965	0,973	0,985	0,975
9D	R_C	0,425	0,553	0,613	0,553
9D	R_{core}	0,613	0,493	0,553	0,613
9D	R_{bl}	0,973	0,973	0,973	0,993
14D	R_C	0,373	0,321	0,381	0,441
14D	R_{core}	0,210	0,381	0,561	0,553
14D	R_{bl}	0,991	0,981	0,991	0,991

Table 1: Radial location of the intermediate layer

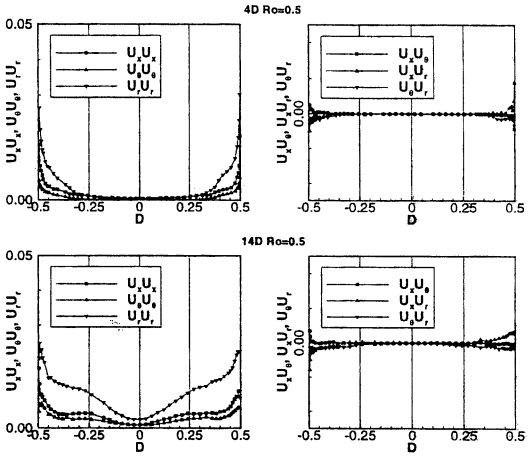

Figure 4: Measured Reynolds stresses at Ro = 0.5

present flow over the range of rotation numbers studied. We wish to draw the readers attention to the very low values of Reynolds shear stresses in the core region even at the large streamwise distance of $x/D = 14$ whereas the Reynolds normal stresses at this station are much higher than at $x/D = 4$. Measurements of the quantities shown as profiles in figs. 3 and 4 over a fine grid in the cross section permit determination of the principal axes of the strain-rate tensor and the Reynolds stress tensor. It is more transparent to employ for this purpose a system of Cartesian coordinates instead of cylindrical coordinates since, with the traversing in the experiment also done likewise, the qualitative nature of the flow may be rendered more directly visible. Fig. 5, which shows with different levels of gray shading the terms of the strain rate tensor and the Reynolds stress tensor for the cases with no swirl and Rotation number 1.0, enables a comparison of the orientation between the two. It is seen that in the swirling flow the areas with higher Reynolds stress, particularly, are rotated with respect to those of higher. This is not so in the flow with zero swirl. To gain further insight into the physical mechanisms responsible for the observed behaviour we view the measured data in the framework of a simple theory for swirling flows. One especially well suited for this purpose in the present context is in Batchelor (1967), vide Chap. 7.5, since this is derivable directly from Euler's equations of motion, holds for rotational flow and establishes an algebraic relation between quantities measured experimentally in this work. According to this theory, in a steady axisymmetric flow with swirl the moment of the azimuthal velocity, i.e. $C = rU_\theta$, remains constant along stream surfaces ψ = constant. Since both C and ψ are evaluable from experiments with little uncertainties, we may examine plots of C against ψ to identify flow regions where this theory provides a satisfactory description of the flow or otherwise. Such plots are given in figs. 6. A cursory glance at these figures shows that C is indeed preserved over streamwise distances as large as $x/D = 14$ for small values of ψ. These are at the core and the result is consistent with the very low values of Reynolds shear stresses observed in the core, cf. fig. 4.

Since, according to this theory the quantity C preserves its value at the initial station, a departure from the same is tantamount to the flow realised in the experiment not conforming to the conditions of derivation of the theory. A closer examination shows Reynolds stresses to be the only factor neglected in the derivation, so the value of ψ at which C departs from its value at the initial station, which we chose here to be $x/D = 4$, pinpoints to the location at which turbulent

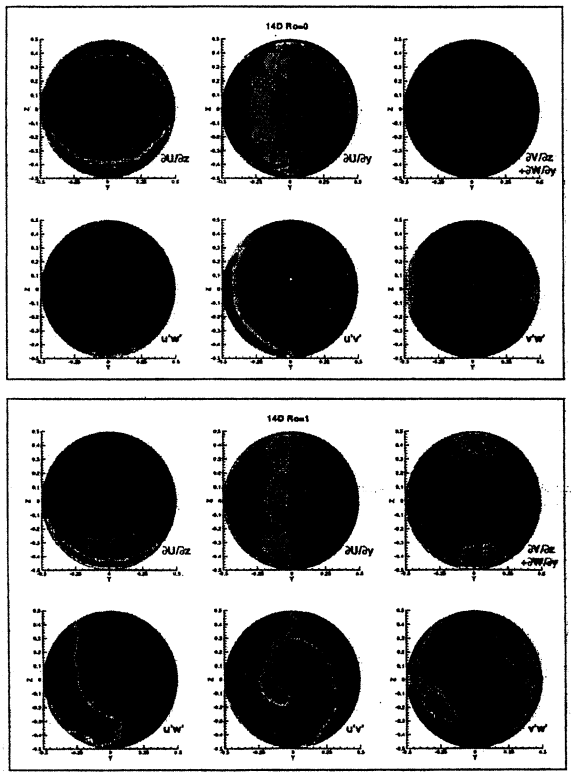

Figure 5: Strain rate and Reynolds stress terms: comparison between Ro = 0 and Ro = 1.0

shear stresses start becoming effective. The radii corresponding to these values of ψ are also given in Table 1 and these may be compared with the radii delineating the boundary layer from the core on the basis of the azimuthal velocity distribution departing from the solid body rotation. In Table 1 we have also given the location of the edge of the wall boundary layer as discernible from the profiles of the azimuthal velocity distributions plotted in fig. 3. We observe that while the radial locaton of the core periphery and C departing from its value at the initial station lie close to each other, the edge of the wall boundary is clearly distinct and closer to the wall. There is thus an intermediate layer separating the core from the wall boundary layer. It is worthy of note that the infliction points in the axial velocity profiles and the "plateaus" in the Reynolds normal stresses are within this intermediate layer.

ACKNOWLEDGEMENTS

Work reported in this paper has been supported by the Deutsche Forschungsgemeinschaft (DFG).

The authors wish to thank Frau D. Mertens and Herrn H. Kocherscheidt for their help in the preparation of this paper.

REFERENCES

Anwer, M. and So, R. M., 1989, "Rotation effects on a fully developed turbulent pipe flow", Experiments in Fluids, Vol. 8, pp. 33-40.

Batchelor, G.K., 1967, An Introduction to Fluid Dynamics, Cambridge University Press.

Budwig, R., 1994, "Refractive index matching methods for liquid flow investigations", Experiments in Fluids, Vol. 17, pp. 350-355.

Escudier, M., 1988, "Vortex breakdown: Observations and explanations", Progress in Aerospace Sciences, Vol. 25, pp. 189-229.

Hogg, S. and Leschziner, M., 1989, "Computation of highly swirling confined flow with a Reynolds stress turbulence model", AIAA Journal, Vol. 27, pp. 57-63.

Kiel, R., 1995, "Experimentelle Untersuchung einer Strömung mit beheiztem lokalem Ablösewirbel an einer geraden Wand", Dr.-Ing. Thesis, Fakultät für Maschinenbau, Ruhr-Universität Bochum, Bochum, Germany, Published in the series Fortschrittberichte, Reihe 7, Nr. 281.

Kitoh, O., 1991, "Experimental study of turbulent swirling flow in a straight pipe", Journal of Fluid Mechanics, Vol. 225, pp. 445-479.

Leuchter, O., Benoit, J.P., Bertoglio, J.P. and Mathieu, J., 1991, "Experimental and theoretical investigation of a homogeneous tubulent shear flow", Advances in Turbulence 3 (Editors: Johansson, A.V. and Alfredsson, P.H.), Springer-Verlag Berlin, Heidelberg, pp .435-444.

Rocklage-Marliani, G., 1998, "Dreidimensionale Laser-Doppler-Anemometrie in drallbehafteter turbulenter Rohrströmung", Dr.-Ing. Thesis, Fakultät für Maschinenbau, Ruhr-Universität Bochum, Bochum, Germany.

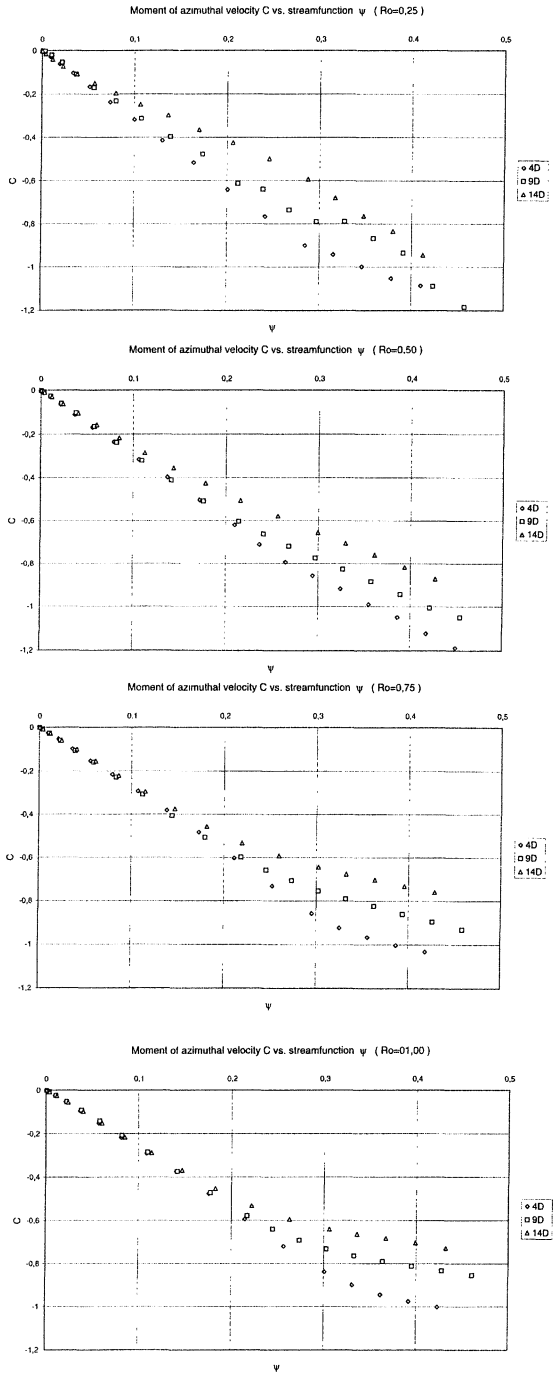

Figure 6: Plots of moment of azimuthal velocity, C, against stream function, ψ